Entrance Region Flow of the Bingham Fluid in a Circular Pipe

S. S. CHEN, L. T. FAN, and C. L. HWANG

Kansas State University, Manhattan, Kansas

The laminar, isothermal entrance region flow of the Bingham fluid in a circular pipe is studied at first by using the momentum integral method and the boundary-layer equation for the Bingham fluid. In addition to the velocity boundary layer, the existence of the shear stress boundary layer is considered. The solution is valid only near the entry because of limitation of the boundary-layer model. The Campbell-Slattery method originally devised for the Newtonian fluid is also used to analyze the Bingham entrance region flow. The results are compared with those obtained through the use of the momentum integral method and those obtained through the use of the variational method by other investigators. While the results obtained in this work appear to be generally reasonable and valid, the results by the other investigators have been found to be somewhat erroneous.

The entrance region flows of the Newtonian fluid and the power law fluid have been studied extensively by using various approximate methods. A thorough review of the literature on the hydrodynamic entrance region flow has been made by Fan and Hwang (*1*). As to the Bingham entrance region flow, the only published work is that by Michiyoshi et al. (*2*), in which the variational method is employed. Their work appears to contain several major inconsistencies. The purpose of this paper is to analyze the entrance region flow of the Bingham fluid by using the classical momentum integral method by Schiller (*3*) and the Campbell-Slattery method (*4*) which was successfully employed for the Newtonian case.

Consider that a Bingham fluid enters a horizontal circular pipe from a large chamber as shown in Figure 1 under the conditions that the flow is steady, laminar, isothermal, and asymmetric, and that the fluid has constant physical properties.

The boundary-layer equation of the Bingham fluid can be written as (5)

$$\frac{1}{r}\frac{\partial}{\partial r}(rv_r) + \frac{\partial v_z}{\partial z} = 0 \tag{1}$$

$$v_r\frac{\partial v_z}{\partial r} + v_z\frac{\partial v_z}{\partial z} = -\frac{1}{\rho}\frac{dp}{dz} - \frac{1}{\rho r}\frac{\partial}{\partial r}(r\tau_{rz}) \tag{2}$$

where

$$\tau_{rz} = -\left\{\mu_0 + \frac{\tau_0}{\left|\frac{\partial v_z}{\partial r}\right|}\right\}\frac{\partial v_z}{\partial r} \tag{3}$$

The boundary conditions are:

1. The velocity components v_r and v_z are zero at the solid wall.
2. In the region beyond the edge of the boundary layer and in the plug-flow region, the velocity derivatives are zero.
3. The velocity at the conduit entrance is uniform, that is, $v_z = \overline{u} = U$, $v_r = 0$, at $z = 0$.
4. Far from the entry, the velocity profile becomes fully developed.

It is worth noting that in addition to the velocity boundary layer there exists a shear stress boundary layer for the flow of the Bingham fluid as shown in Figure 2. At the edge of the velocity boundary layer the velocity gradient is zero, while at the edge of the shear stress boundary layer, which is thicker than the velocity boundary layer, the shear stress becomes zero.

THE MOMENTUM INTEGRAL METHOD

The momentum integral method for the entrance region flow of Newtonian fluid was first developed by Schiller (*3*). He assumed a parabolic velocity profile in the boundary layer with a thickness $\delta(z)$ and a uniform velocity profile outside the boundary layer. From the form of the velocity profile in the fully developed region as shown in Figure 3, it appears that the momentum integral method can also be used to analyze the entrance region flow of the Bingham fluid because the uniform velocity distribution outside the boundary layer is analogous to the plug-flow region of the Bingham flow. Hence it may be expected that this model can describe correctly the flow characteristics of the Bingham fluid in the entrance region.

It is assumed that the pressure gradient can be related to the plug-flow velocity by

$$U\frac{dU}{dz} = -\frac{1}{\rho}\frac{dp}{dz} \tag{4}$$

where U is a function of z. Substituting Equation (4) into Equation (2) and integrating the resulting equation with respect to r from $r = R$ at the solid wall to $r = R - \delta_s$ at the edge of the shear stress boundary layer, where no shear stress exists, we have [see Appendix 1]*

$$\frac{dU}{dz}\int_R^{R-\delta_s}(U - v_z)\,rdr + \frac{d}{dz}\int_R^{R-\delta_s} v_z(U - v_z)\,rdr = -\frac{R}{\rho}\tau_w \tag{5}$$

* Appendixes 1 through 8 have been deposited as document 00769 with the ASIS National Auxiliary Publications Service, c/o CCM Information Sciences, Inc., 22 W. 34th St., New York 10001 and may be obtained for $1.00 for microfiche or $3.00 for photocopies.

where

$$\tau_w = [\tau_{rz}|_{r=R}] = -\mu_0 \left(\frac{\partial v_z}{\partial r}\right)_{r=R} + \tau_0$$

Since $U - v_z$ becomes zero outside the velocity boundary layer $r = \delta$, Equation (5) becomes

$$\frac{dU}{dz}\int_R^{R-\delta} (U - v_z)rdr + \frac{d}{dz}\int_R^{R-\delta} v_z(U - v_z)rdr = \frac{R\mu_0}{\rho}\left(\frac{\partial v_z}{\partial r}\right)_{r=R} - \frac{R\tau_0}{\rho} \quad (6)$$

As in the case of Newtonian entrance region flow, the following parabolic form of velocity distribution inside the boundary layer is assumed to be

$$\frac{v_z}{U} = 2\left(\frac{y}{\delta}\right) - \left(\frac{y}{\delta}\right)^2 \quad (7)$$

where y is the new coordinate as shown in Figure 1 and defined by

$$y = R - r \quad (8)$$

Substituting the assumed velocity profile Equation (7) into Equation (6) and carrying out the integration, we have in dimensionless form (see Appendix 2)†

$$\delta^* U^* \left(\frac{3}{5} - \frac{11}{60}\delta^*\right)\frac{dU^*}{dz^*} + U^{*2}\left(\frac{2}{15} - \frac{1}{10}\delta^*\right)\frac{d\delta^*}{dz^*} = 2\frac{U^*}{\delta^*} + \tau_0^* \quad (9)$$

The relation between the boundary-layer thickness δ and the center core velocity U can be obtained by using the macroscopic mass balance and given by (see Appendix 3)†

$$\delta^{*2} - 4\delta^* = 6\left(\frac{1}{U^*} - 1\right) \quad (10)$$

Solving Equation (10) for δ^* and noting that $\delta^* < 1$ and $U^* \geq 1$, we obtain

$$\delta^* = 2 - \sqrt{\frac{6}{U^*} - 2} \quad (11)$$

Equation (9) now reduces to a first-order differential equation if the relation of δ^* and U^* in Equation (11) is used:

$$\left(\frac{5}{6}U^* + \frac{2}{15}U^*D - \frac{1}{5D} - \frac{4}{5}\right)\frac{dU^*}{dz^*} = \frac{2U^*}{2 - D} + \tau_0^* \quad (12)$$

where

$$D = \sqrt{\frac{6}{U^*} - 2}$$

The initial condition of Equation (12) is

$$U^* = 1 \quad \text{at} \quad z^* = 0 \quad (13)$$

Equation (12) can be integrated numerically by using any standard method of numerical integration. The solution of Equation (12) will give the relation between the dimensionless center velocity U^* and the dimensionless tube length z^* for a given value of τ_0^*. Using the relationship of δ^* and U^* given by Equation (11) and the velocity profile given by Equation (7), we can also calculate δ^* and the velocity distribution for a given z^* and τ_0^*.

To obtain a clear visualization of the characteristics of the Bingham flow, it is preferable to use the dimensionless plug-flow radius $r_0^* = r_0/R$ in place of the dimensionless yield stress τ_0^* as a parameter. The relation between r_0^* and τ_0^* can be obtained from the expression of the average velocity in fully developed tube flow as

$$\tau_0^* = \frac{12r_0^*}{3 - 4r_0^* + r_0^{*4}} \quad (14)$$

For each r_0^* there exists a corresponding τ_0^* which is called the *plasticity number* or *Bingham number*. When r_0^* is zero, the fluid is Newtonian. When r_0^* approaches unity, τ_0^* is infinite corresponding to the plug flow. Thus r_0^* may be used as a parameter together with the Reynolds number N_{Re} in the Bingham flow.

The entrance length z_e is the distance from the tube inlet to the point downstream where the boundary-layer velocity profile asymptotically approaches that of the fully developed flow. In other words, at $z = z_e$, the boundary-layer thickness δ_e is equal to $R - r_0$, and the center velocity U_e is equal to the velocity in the fully developed plug-flow region. Using dimensionless quantities, we obtain

$$\delta_e^* = 1 - r_0^* \quad (15)$$

$$U_e^* = \frac{6}{3 + 2r_0^* + r_0^{*2}} \quad (16)$$

For each given r_0^*, we can calculate U_e^* from Equation (16). The corresponding dimensionless entrance length z_e^* is then obtained by utilizing Equation (12).

The pressure drop $|\Delta p|$ from the tube inlet to any section in the entrance region can be obtained by integrating Equation (4):

$$|\Delta p^*| = p_0^* - p^* = U^{*2} - 1 \quad (17)$$

Therefore, the pressure drop in the entrance region $|\Delta p_e^*|$ can be expressed in terms of dimensionless center velocity at $z = z_e$:

$$|\Delta p_e^*| = p_0^* - p_e^* = U_e^{*2} - 1 \quad (18)$$

For the purpose of comparison, the dimensionless pressure drop based on the fully developed region for tube length Δz^* as shown in Figure 4 is (see Appendix 4)†

$$|\Delta p_f^*| = \frac{48\Delta z^*}{3 - 4r_0^* + r_0^{*4}} = \frac{48(z^* - z_e^*)}{3 - 4r_0^* + r_0^{*4}} \quad (19)$$

Note that $|\Delta p_f^*|$ increases with r_0^* for a given Δz^*. Therefore, the pressure drop from the tube entry to any cross section z^* in the fully developed region is customarily defined as

$$|\Delta p^*| = \frac{48z^*}{3 - 4r_0^* + r_0^{*4}} + C \quad (20)$$

where the correction factor C is

$$C = U_e^{*2} - 1 - \frac{48z_e^*}{3 - 4r_0^* + r_0^{*4}} \quad (21)$$

Numerical Procedures and Results

The computational procedure is as follows:

1. Given a value of plug-flow radius r_0^*, the corresponding yield stress τ_0^* can be calculated from Equation (14). The results are shown in Figure 5. In the following numerical procedure, r_0^* in the range from 0 to 0.9 is used as the parameter.

2. The relationship between center velocity U^* and tube distance z^* can be obtained by numerical integration of Equation (12) by using the trapezoidal rule. The results are shown in Figure 6.

† See footnote on p. 293.

† See footnote on column 1.

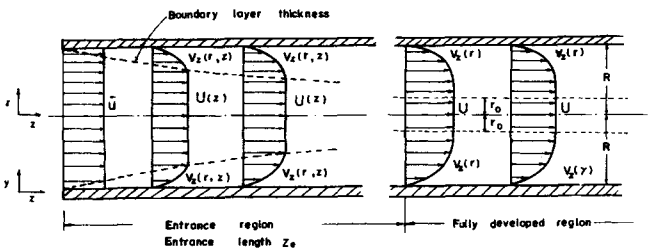

Fig. 1. Entrance region and fully developed region of the Bingham fluid in a circular pipe.

3. For given values of U^*, the corresponding boundary-layer thickness δ^* can be obtained from Equation (11). Thus the relationship between δ^* and z^* is established by using step 2 and Equation (11), and the results are shown in Figure 7.

4. The velocity profile at a given z^* is then calculated from Equation (7). The results for the case of $r_0^* = 0.2$ are shown in Figure 8.

5. The entrance length z_e^* is obtained in step 2 when U^* approaches the fully developed center velocity U_e^*, which can be calculated from Equation (16). The entrance length z_e^* is plotted against r_0^* in Figure 9.

6. The pressure drop from the tube entry to any cross section downstream in the entrance region is obtained from Equation (17). The results are shown in Figure 10.

7. The correction factor defined in Equation (21) can be calculated for given values of r_0^*. The results are plotted in Figure 11.

Discussion

The characteristic behavior of the Bingham fluid is that it remains rigid when the shear stress is less than the yield stress but flows when the shear stress is larger than the yield stress. This flow behavior implies that there always exists a true plug-flow region outside the boundary layer if the yield stress is not zero. At the edge of the boundary layer the velocity gradient $\partial v_z/\partial r$ is zero, and the shear stress τ_{rz} is equal to the yield stress τ_0, as can be visualized from Equation (3). The fluid outside the boundary layer flows like a solid body with elastic properties because the fluid is under stress τ_0 at the edge of the boundary layer. This consideration prompted us to study the Bingham entrance region flow problem using the momentum integral method.

The center-line velocity U^* is plotted against z^* for each r_0^* (see Figure 6) does not approach the fully developed value asymptotically. This results in shorter entrance lengths (see Figure 9) compared with those obtained from the Campbell-Slattery method and the variational method, which will be described later. As shown in Figures 6 and 7, the center-line velocity and boundary-layer thickness increase with increasing r_0^* at a given tube length z^*, but near the tube entry $z^* = z/RN_{Re} < 0.02$ the variation of U^* and δ^* for different values of r_0^* is very small. Figure 9 indicates that the entrance length z_e^* decreases with increasing r_0^*.

SOLUTION BY THE CAMPBELL-SLATTERY METHOD

The unrealistic results in the region far from the entry $z^* > 0.04$ obtained from the momentum integral method for Newtonian fluids were corrected by Campbell and Slattery (4). In addition to the basic assumptions employed in the momentum integral method, they used the macroscopic mechanical energy balance to account for viscous dissipation within the boundary layer. Their results are good in overall description of the velocity field within

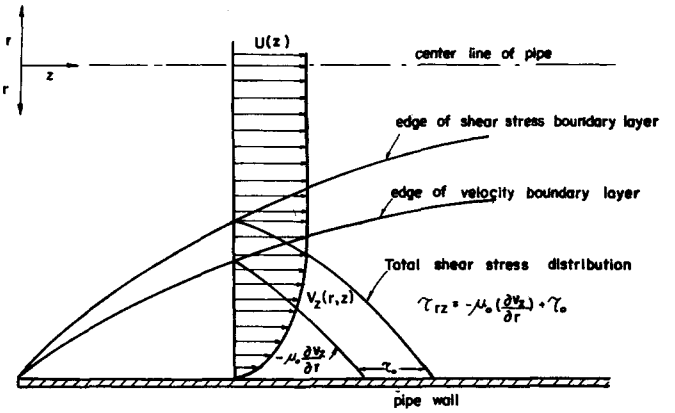

Fig. 2. Shear stress boundary layer and velocity boundary layer for the Bingham fluid in the entrance region of a circular pipe.

the entrance region. The method of correction by Campbell and Slattery originally developed for Newtonian flow will be applied to Bingham fluids in this section.

The macroscopic momentum balance in the entrance region of a pipe may be written (6) as

$$\Delta(\rho \langle v_z^2 \rangle S + pS) + F = 0 \tag{22}$$

where $\langle v_z^P \rangle$ is defined as

$$\langle v_z^P \rangle = \int_0^{2\pi} \int_0^R v_z^P \, r dr d\theta \Big/ \int_0^{2\pi} \int_0^R r dr d\theta = \frac{\int_0^{2\pi} \int_0^R v_z^P \, r dr d\theta}{S} \tag{23}$$

Here it is assumed that $v_z^2 >> v_r^2$. If Equation (22) is applied to a differential length dz, we have (see Appendix 5) †

$$\rho \frac{d}{dz} \int_0^R v_z^2 \, r dr + \frac{R^2}{2} \frac{dp}{dz} + [\tau_{rz}]_{r=R} R = 0 \tag{24}$$

The assumed forms of the velocity distribution inside the boundary layer given by Equation (7) can be used in performing the integration of $\int_0^R v_z^2 \, r dr$ and in calculating the shear stress at the wall $[\tau_{rz}]_{r=R}$ in Equation (24). The result is

$$\frac{d}{dz^*}\left[U^{*2} \left(\frac{1}{2} - \frac{7}{15}\delta^* + \frac{2}{15}\delta^{*2} \right) \right] + \frac{1}{4} \frac{dp^*}{dz^*} + \frac{U^*}{2\delta^*} + \tau_0^* = 0 \tag{25}$$

The macroscopic mechanical energy balance (6) in the entrance region may be written as

$$\Delta \left(\frac{1}{2} \rho S \langle v_z^3 \rangle \right) + w \int_{p_0}^{p} \frac{dp}{\rho} + E_v = 0 \tag{26}$$

where $w = \rho \langle v_z \rangle S$. Equation (26) can be applied to the fluid from the tube inlet to any cross section in the entrance region:

$$\frac{1}{2}\rho \int_0^R v_z^3 \, r dr - \frac{1}{4}\rho \, \bar{u}^3 R^2 + p \int_0^R v_z \, r dr - \frac{1}{2} p_0 \, \bar{u} \, R^2 + \frac{E_v}{2\pi} = 0 \tag{27}$$

† See footnote on p. 293.

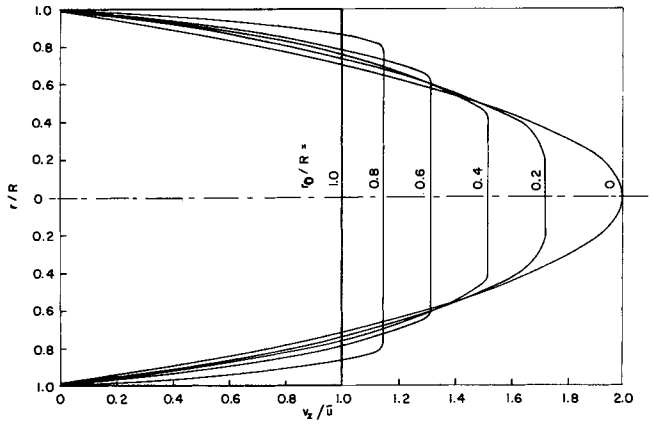

Fig. 3. Fully developed velocity profiles of the Bingham fluid in pipes.

where

$$E_v = -\int_0^z \int_0^{2\pi} \int_0^R (\tau : \nabla v)\, r dr d\theta dz \qquad (28)$$

Using the scalar or expanded expression of $(\tau : \nabla v)$ (6) and the usual boundary-layer assumptions, that is, neglecting the small term of velocity derivatives except $\partial v_z/\partial r$, we have

$$-(\tau : \nabla v) = \left(\mu_0 - \frac{\tau_0}{\frac{\partial v_z}{\partial r}}\right)\left(\frac{\partial v_z}{\partial r}\right)^2 \qquad (29)$$

Equation (28) can be integrated with respect to r and θ by using the expression of Equation (29) and the assumed

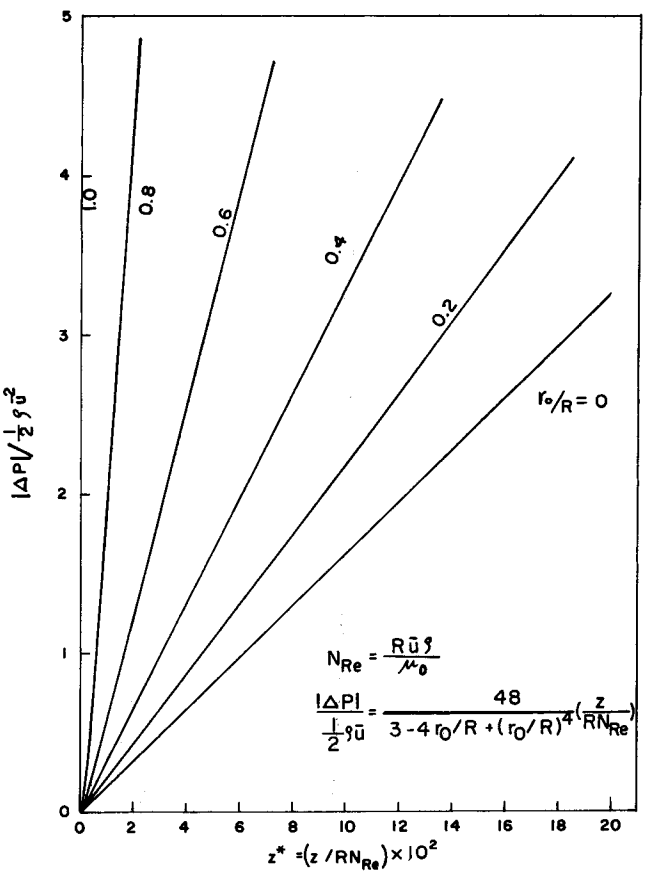

Fig. 4. Fully developed pressure drop vs. tube length for the Bingham fluid.

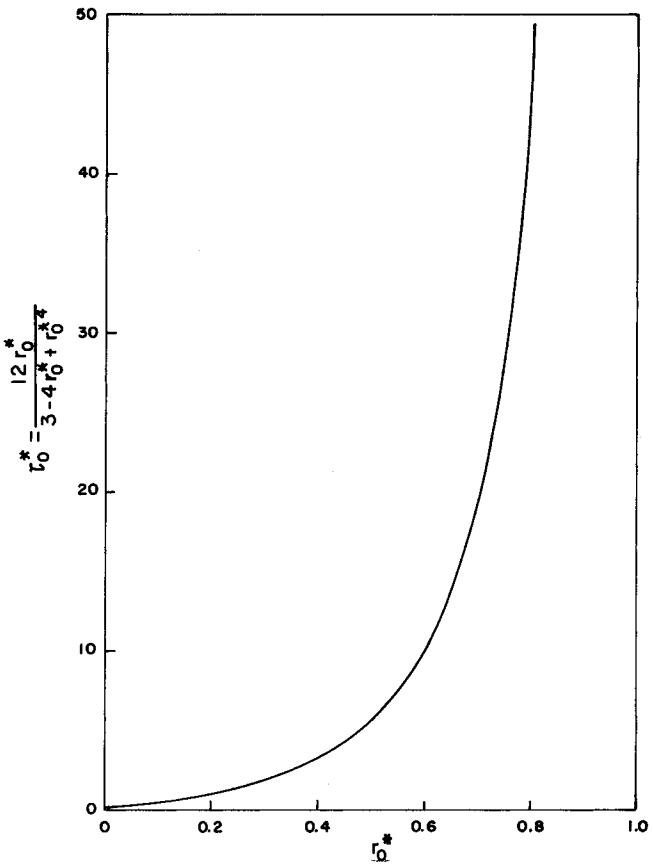

Fig. 5. Yield stresses of the Bingham fluid as a function of plug-flow radius.

form of the velocity profile. The result is (see Appendix 6)†

$$E_v = 2\pi\mu_0 \int_0^z U^2 \left(\frac{4}{3}\frac{R}{\delta} - \frac{1}{3}\right) dz - 2\pi\tau_0 \int_0^z U\left(\frac{\delta}{3} - R\right) dz \qquad (30)$$

Combining Equations (27) and (30) and differentiating the resulting equations with respect to z, we have (see Appendix 7)†

$$\frac{1}{4}\frac{dp^*}{dz^*} = -\frac{1}{2}\frac{d}{dz^*}\left[U^{*3}\left(\frac{1}{2} - \frac{19}{35}\delta^* + \frac{47}{280}\delta^{*2}\right)\right] - U^{*2}\left(\frac{4}{3}\frac{1}{\delta^*} - \frac{1}{3}\right) + U^*\,\tau_0^*\left(\frac{1}{3}\delta^* - 1\right) \qquad (31)$$

Elimination of the pressure gradient dp^*/dz^* between Equations (25) and (31) gives

$$\frac{d}{dz^*}\left[U^{*2}\left(\frac{1}{2} - \frac{7}{15}\delta^* + \frac{2}{15}\delta^{*2}\right)\right] - \frac{1}{2}\frac{d}{dz^*}\left[U^{*3}\left(\frac{1}{2} - \frac{19}{35}\delta^* + \frac{47}{280}\delta^{*2}\right)\right] - U^{*2}\left(\frac{4}{3}\frac{1}{\delta^*} - \frac{1}{3}\right) + \frac{2U^*}{\delta^*} + \tau_0^*\left[1 + U^*\left(\frac{1}{3}\delta^* - 1\right)\right] = 0 \qquad (32)$$

The center velocity U^* can be expressed in terms of the

† See footnote on p. 293.

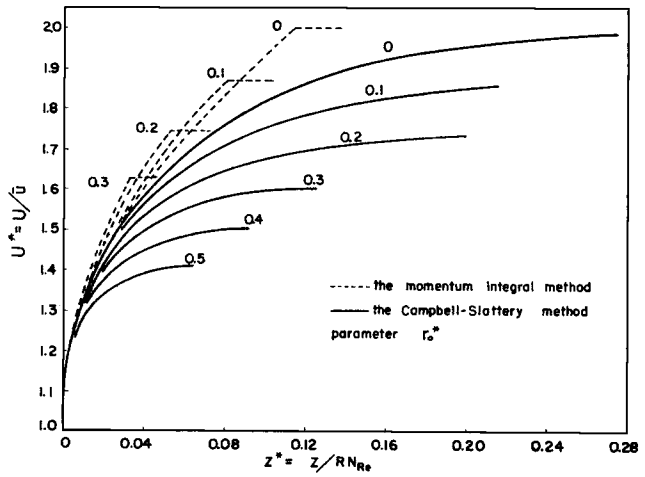

Fig. 6. Center-core velocity of the Bingham fluid as a function of tube distance by the momentum integral method and the Campbell-Slattery method.

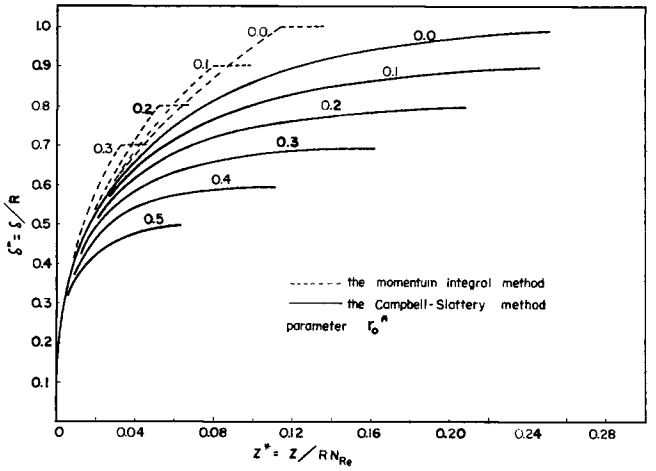

Fig. 7. Boundary-layer thickness of the Bingham fluids as a function of tube length by the momentum integral method and the Campbell-Slattery method.

boundary-layer thickness by

$$U^* = \frac{6}{\delta^{*2} - 4\delta^* + 6} \tag{33}$$

Using Equation (33), we can eliminate U^* from Equation (32) and carry out the differentiation of the resulting equation to obtain (see Appendix 8)†

$$\delta^* (112\delta^{*5} - 1{,}036\delta^{*4} + 3{,}130\delta^{*3} - 3{,}574\delta^{*2} + 1{,}014\delta^* + 432)\frac{d\delta^*}{dz^*} = 140 (\delta^{*6} - 118\delta^{*5} + 54\delta^{*4} - 148\delta^{*3} + 236\delta^{*2} - 204\delta^* + 72) + \frac{35}{3}\tau_0^* \delta^{*2} (\delta^{*7} - 14\delta^{*6} + 94\delta^{*5} - 340\delta^{*4} + 812\delta^{*3} - 1{,}224\delta^{*2} + 1{,}080\delta^* - 432) \tag{34}$$

Equation (34) is the differential equation which determines the relationship between δ^* and z^*. The boundary condition is $\delta^* = 0$ at $z^* = 0$. For Newtonian fluids $\tau_0^* = 0$, Equation (34) can be integrated analytically (*4*). Equation (32) reduces to the differential equation which relates U^* to z^* if Equation (11) is used. The boundary condition is $U^* = 1$ at $z^* = 0$. Entrance length z_e^* is determined by the numerical integration of the resulting differential equation at $U^* = U_e^*$.

The pressure drop in the entrance region can be obtained by integrating either Equation (25) or (31) from the tube inlet to any cross section in the entrance region:

$$|\Delta p^*| = 4\left\{ U^{*2}\left(\frac{1}{2} - \frac{7}{15}\delta^* + \frac{2}{15}\delta^{*2}\right) - \frac{1}{2} + 2\int_0^{z^*} \frac{U^*}{\delta^*} dz^* + \tau_0^* z^* \right\} \tag{35}$$

or

$$|\Delta p^*| = 2U^{*3}\left(\frac{1}{2} - \frac{19}{35}\delta^* + \frac{47}{280}\delta^{*2}\right) - 1 + \frac{4}{3}\int_0^{z^*} U^{*2}\left(\frac{4}{\delta^*} - 1\right) dz^* + \frac{4}{3}\tau_0^* \int_0^{z^*} U^*(3 - \delta^*) dz^* \tag{36}$$

If the expression of Equation (35) is used to calculate the pressure drop, the correction factor becomes

$$C = 4\left\{ U_e^{*2}\left(\frac{1}{2} - \frac{7}{15}\delta_e^* + \frac{2}{15}\delta_e^{*2}\right) - \frac{1}{2} + 2\int_0^{z_e^*} \frac{U^*}{\delta^*} dz^* + \tau_0^* z_e^* \right\} - \frac{48 z_e^*}{3 - 4r_0^* + r_0^{*4}} \tag{37}$$

The numerical procedure is, in general, similar to that in the momentum integral method. The determination of pressure drop as a function of z^* needs an additional integration. The center velocity and boundary-layer thickness as shown in Figures 6 and 7 as functions of tube length are obtained by numerical integration of Equation (34) combined with Equation (33). The entrance lengths (99% criterion) are plotted against r_0^* in Figure 9. Pressure drop calculated from Equation (35) is shown in Figure 10, and correction factor C from Equation (37) is shown in Figure 11.

Results and Discussion

Since the present investigation is the first work applying the Campbell-Slattery method (*4*) originally developed for the Newtonian entrance region flow to the Bingham fluid, the numerical results obtained are compared with those obtained by the momentum integral method presented in the preceding section and with the variational method (*2*). Although the plug-flow velocity and boundary-layer thick-

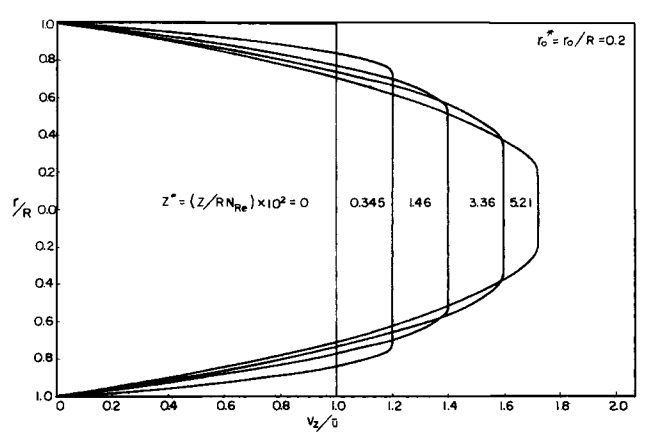

Fig. 8. Velocity profiles of the Bingham fluid in the entrance region by the momentum integral method.

† See footnote on p. 293.

ness plotted against pipe length for different values of plug-flow radius indicate the opposite trend with respect to increasing plug-flow radius as compared with those of the momentum integral method, both plug-flow velocity and boundary-layer thickness from this work approach the fully developed values asymptotically. Furthermore, the pressure drops in the entrance region are in good agreement with the results from the momentum integral method as shown in Figure 10. The results of pressure drop from the momentum integral method and the Campbell-Slattery method are also compared with those from the variational method in Figure 12. The entrance lengths and correction factors for different values of r_0^* as shown in Figures 9 and 11 are in general longer and higher than those obtained from the momentum integral method and variational method.

It should be pointed out that the validity of the approximate form of equation of motion used in the variational method by Michiyoshi et al. (2) is doubtful. They used the boundary-layer approximation to arrive at the following two expressions:

$$\frac{\partial v_z}{\partial z} \approx -\frac{\partial v_r}{\partial r} \tag{38}$$

and

$$\sqrt{\frac{1}{2}(\mathbf{\Delta} : \mathbf{\Delta})} \approx \frac{\partial v_z}{\partial r} + 2\frac{\partial v_r}{\partial r} \tag{39}$$

Under these two approximations they concluded that the equation of motion can be simplified as

$$v_r\frac{\partial v_z}{\partial r} + v_z\frac{\partial v_z}{\partial z} = -\frac{1}{\rho}\frac{dp}{dz} + \frac{\mu_0}{\rho}\left(\frac{\partial^2 v_z}{\partial r^2} + \frac{1}{r}\frac{\partial v_z}{\partial r}\right) + \frac{\tau_0}{\rho}\frac{\partial}{\partial r}\left\{\frac{\partial v_z/\partial r}{\frac{\partial v_z}{\partial r} + 2\frac{\partial v_r}{\partial r}}\right\} \tag{40}$$

Furthermore, they made an additional assumption that

$$\frac{\partial v_z}{\partial r} \approx \left(\frac{\partial v_z}{\partial r} + 2\frac{\partial v_r}{\partial r}\right) \tag{41}$$

The reduction of the equation of motion to Equation (40) based on Equations (38) and (39) cannot be achieved according to the derivation given in reference 5.

CONCLUSION

The theoretical analysis of the entrance region flow of the Bingham fluid in a circular pipe was first presented by Michiyoshi et al. (2), using the variational method. The method involved the boundary-layer simplifications and variational arguments. The validity of simplifications and arguments needs further verification. First of all, the starting form of the governing equation used by the variational method should be modified. The proposed velocity profile used in their method would not provide the reasonable flow behavior of the Bingham fluid. Furthermore, the method requires an excessive mathematical manipulation. The results of their analysis can not be justified with two experimental pressure drop data obtained by them.

For the entrance length and pressure drop correction factors, the results from the variational method show a reasonable trend, that is, both decrease with increasing plug-flow radius. The pressure drop curves for various plug-flow radii cross each other in the entrance region and in the fully developed region. This phenomenon may contradict the actual physical situation.

Solutions of the governing equations obtained in this work by using the momentum integral method and the Campbell-Slattery method, especially those by the second method, appear to conform to the characteristics of the Bingham fluid.

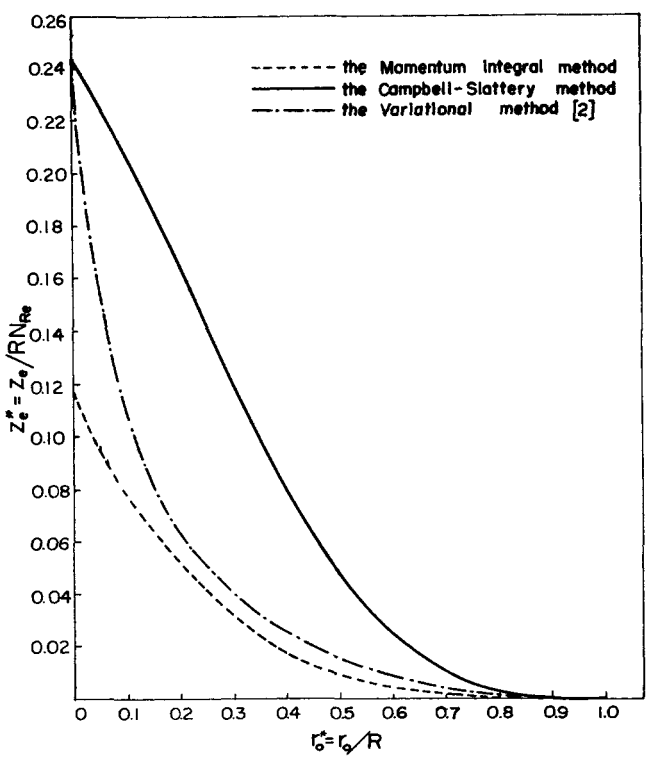

Fig. 9. Entrance length of the Bingham fluid as a function of plug-flow radius by various methods.

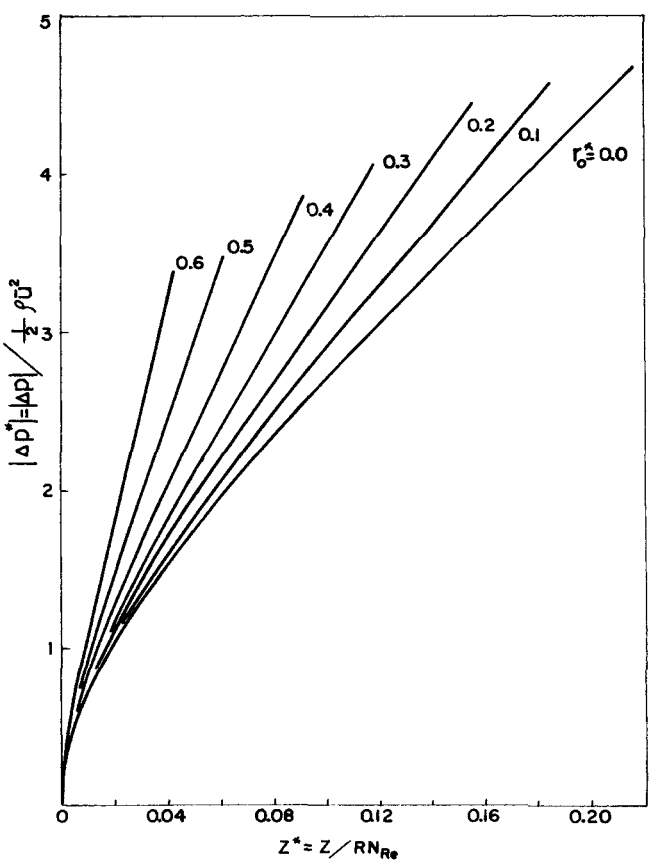

Fig. 10. Pressure drop of the Bingham fluid as a function of pipe length by the momentum integral method ($Z^* < Z^*_e$) and the Campbell-Slattery method.

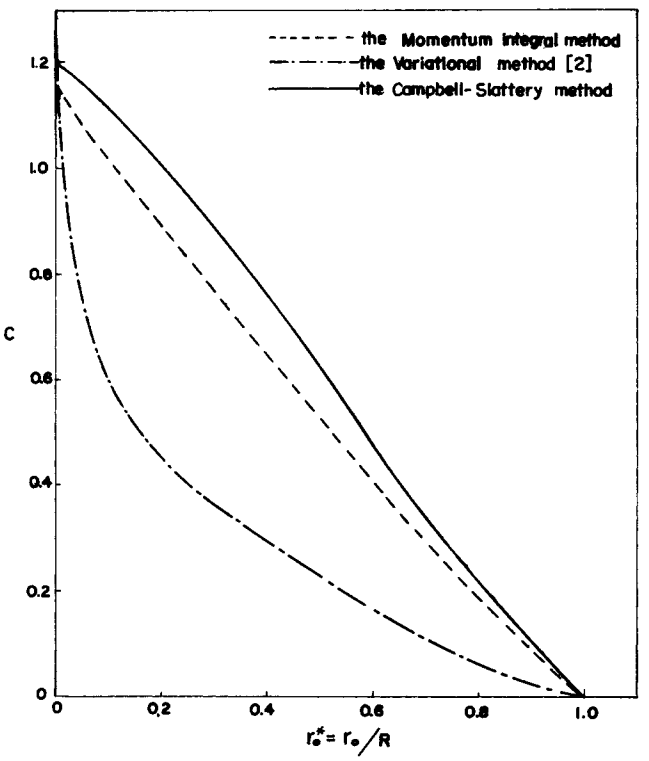

Fig. 11. Correction factor of Bingham fluids as a function of plug-flow radius by various methods.

The momentum integral method is historically important in the study of the boundary layer. The results obtained by the momentum integral method appear to provide a reasonable overall description of the Bingham flow in the entrance region except a certain specific point discussed earlier.

The Campbell-Slattery method for Newtonian entrance region flow problems has been accepted as a successful approach and is discussed in detail in their paper. The curves of entrance length and pressure drop correction factor for the Bingham fluid show the same trend but are somewhat higher than those from the variational method. The pressure drop curves in the entrance region have no crossing between each other and are consistent with the case of fully developed flow, that is, the pressure drop is higher for higher plug-flow radius. Therefore, we may conclude that a solution by the Campbell-Slattery method which involves less mathematical manipulation provides a valid overall description of flow characteristics of the Bingham fluid in the entrance region of a circular pipe.

ACKNOWLEDGMENT

This study was supported by the Air Force Office of Scientific Research Grant AFOSR-68-1410.

NOTATION

C = pressure correction factor

$D = \sqrt{\frac{6}{U^*} - 2}$

E_v = rate of irreversible conversion of mechanical to internal energy defined by Equation (28)

F = friction force of the fluid on the tube wall

N_{Re} = Reynolds number, $R\bar{u}\rho/\mu_0$

P = constant defined by Equation (23)

p = pressure

p_0 = pressure at the entry

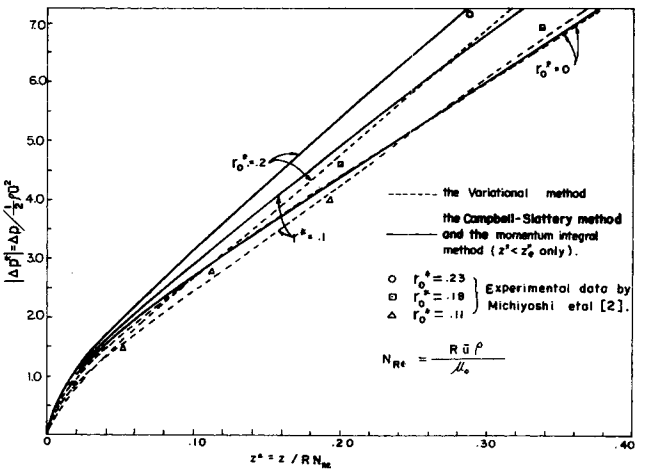

Fig. 12. Comparison of pressure drops of the Bingham fluid calculated from the Campbell-Slattery method, the momentum integral method, and the variational method.

p^* = $p/\frac{1}{2}\rho\bar{u}^2$

p_0^* = dimensionless pressure at tube entry

$|\Delta p^*|$ = $p_0^* - p^*$

R = pipe radius

r = radial coordinate

S = cross-sectional area of a pipe

U = velocity outside boundary layer

U^* = dimensionless velocity outside boundary layer, $U/\bar{u}$

$\bar{u}$ = average velocity

$\underline{v}$ = velocity vector

v_r, v_z = r and z components of velocity

w = mass flow rate

y = $R - r$

z = axial distance

z^* = dimensionless axial distance, $z/(RN_{Re})$

Greek Letters

$\blacktriangle$ = rate of deformation tensor

δ = boundary-layer thickness

δ^* = dimensionless boundary-layer thickness, δ/R

θ = cylindrical coordinate

μ_0 = coefficient of rigidity, parameter in the Bingham fluid

ρ = density

$\underline{\tau}$ = shear stress tensor

τ_0 = yield stress, parameter in the Bingham fluid

τ_0^* = Bingham number, $\tau_0 R/\mu_0\bar{u}$

τ_w = shear stress at the wall

Subscript

e = evaluated at the entrance length where the center velocity U reaches the fully developed value

LITERATURE CITED

1. Fan, L. T., and C. L. Hwang, *Special Rept. No. 67*, Engineering Experiment Station, Kan. State Univ., Manhattan (1966).
2. Michiyoshi, L., K. Mizuno, and Y. Hoshinai, *Intern. Chem. Eng.*, **6**, No. 2, 373-381 (1966).
3. Schiller, L., *ZAMM*, **2**, 96-106 (1922).
4. Campbell, W. D., and J. C. Slattery, *Trans. Am. Soc. Mech. Engrs. J. Basic Eng.*, **85D**, 41-46 (1963).
5. Chen, S. S., M.S. thesis, Kan. State Univ., Manhattan (1968).
6. Bird, R. B., W. E. Stewart, and E. N. Lightfoot, "Transport Phenomena," Wiley, New York (1960).

Manuscript received August 1, 1968; revision received September 20, 1968; paper accepted September 23, 1968.